JCTC Journal of Chemical Theory and Computation

Article

pubs.acs.org/JCTC

Free Energy Calculations with Reduced Potential Cutoff Radii

Stuart J. Davie,[†] James C. Reid,[†,‡] and Debra J. Searles*[,†,‡,§]

[†]Queensland Micro- and Nanotechnology Centre and School of Biomolecular and Physical Sciences, Griffith University, Brisbane, Queensland 4111, Australia

[‡]Australian Institute for Bioengineering and Nanotechnology, The University of Queensland, Brisbane, Queensland 4072, Australia

[§]School of Chemistry and Molecular Biosciences, The University of Queensland, Brisbane, Queensland 4072, Australia

ABSTRACT: The Jarzynski Equality, the Crooks Fluctuation Theorem, and the Maximum Likelihood Estimator use a nonequilibrium approach for the determination of free energy differences due to a change in the state of a system. Here, this approach is used in combination with a novel transformation algorithm to increase computational efficiency in simulations with interacting particles, without losing accuracy. The algorithm is shown to work well for a Lennard-Jones fluid undergoing a change in density over three very different density ranges, and for the systems considered the algorithm demonstrates computational savings of up to approximately 90%. The results obtained directly from the Jarzynski Equality and from the Maximum Likelihood Estimator are also compared.

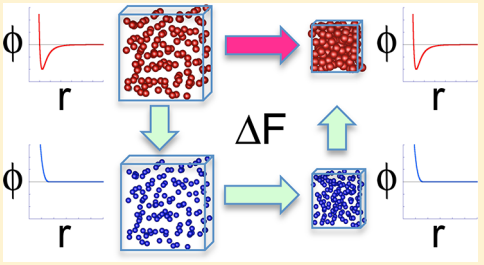

INTRODUCTION

Traditionally, in order to use molecular dynamics simulations to calculate the free energy difference between two equilibrium states of a system, partition function calculations, quasi-static changes, or thermodynamic integration have been used. These all involve calculations of systems in equilibrium, and we therefore refer to them as "equilibrium methods." The discovery of the Jarzynski Equality (JE) in 1997 allowed the calculation of free energy differences from an exponential average of transformations which could be completed at an arbitrary speed,[1,2] so the system is not maintained at equilibrium throughout the transformation. Jarzynski found that the free energy difference between two equilibrium states, sampled from canonical distributions with the same number of particles, volume, and temperature, is related to an ensemble average of an exponential function of the work required to drive the system from a microstate of state 1 to a microstate of state 2, $w_{1\to2}$:

$$\langle e^{-\beta w_{1\to2}}\rangle_1 = e^{-\beta \Delta F_{1\to2}} \tag{1}$$

where $\Delta F_{1\to2}$ is the free energy difference between state 1 and state 2, $\beta = 1/(k_B T)$, k_B is Boltzmann's constant, T is the temperature, and $\langle ... \rangle_1$ represents an ensemble average relative to the equilibrium distribution of state 1.[3] Since the development of the JE, there has been a renewed push to find the most efficient way to measure free energies using nonequilibrium pathways. In addition, algorithms have been developed to treat systems in other ensembles or where the transformation is not just a transformation of the Hamiltonian of the system.

To develop efficient algorithms, work relations based upon the same underlying principles as the JE, including the Crooks Fluctuation Theorem (CFT)[4,5] and the Maximum Likelihood Estimator (MLE) of Shirts et al.,[6,7] were developed for measuring free energy changes when work distributions can be determined for both the forward and reverse processes. The MLE is an iterative free energy calculation method that, by combining the work calculated for a forward transformation with that of the reverse transformation, can often accurately determine free energy differences with significantly increased efficiency over the JE for a finite sized data set. The free energy obtained via the MLE satisfies the expression

$$\sum_{i=1}^{N_{1\to2}} \frac{1}{1+\frac{N_{1\to2}}{N_{2\to1}}\exp(\beta(w_{1\to2,i}-\Delta F))} = \sum_{i=1}^{N_{2\to1}} \frac{1}{1+\frac{N_{2\to1}}{N_{1\to2}}\exp(\beta(w_{2\to1,i}+\Delta F))} \tag{2}$$

where $N_{1\to2}$ is the number of trajectories simulated for the forward process and $N_{2\to1}$ is the number for the reverse process. Here, the JE is used to determine the initial estimate for the iterative process, and we use an equal number of trajectories for both forward and reverse transformations, $N_{1\to2} = N_{2\to1}$, which is generally the most efficient balance of samples for the MLE.[8]

At the same time, research has been carried out on optimizing the pathway to improve nonequilibrium, free energy calculation methods.[9] As the free energy of a system is a state function, it is possible to consider a variety of thermodynamic pathways in order to transform a system from one state to another when calculating free energy differences.

Received: November 1, 2012
Published: March 5, 2013

ACS Publications © 2013 American Chemical Society

Nonphysical pathways have been used in calculation of free energy changes using equilibrium methods for many years. For example, to determine the free energy of a solid, the differences in free energy between the solid and the ideal Einstein crystal are commonly used.[10] The use of nonphysical pathways has also been extensively exploited in order to improve the efficiency of sampling and therefore the calculation of free energy changes.[11] Recently, thermodynamic integration along a nonphysical path has been used in the determination of the solid−liquid melting line of a Lennard-Jones (LJ) fluid, sodium chloride, and benzene[12−15] using equilibrium methods. For nonequilibrium methods, a study by Lechner et al.[16] found that for some processes, the use of large timesteps during the simulation of the nonequilibrium trajectories decreased computation time despite maintaining accuracy. Thus, Lechner et al. demonstrated that for certain systems, free energy changes can be calculated accurately and with increased efficiency through the use of nonphysical transformation techniques. The approach taken here builds on these optimization approaches.

We note that in molecular dynamics simulations, the dominant component of the total computation time is the force calculation, with more sophisticated potentials requiring significantly more computation than simpler potentials. We present a nonequilibrium method where the nonequilibrium pathway goes from a selected potential to a simpler, less computationally demanding, potential and back again, giving the accuracy of the selected potential with the speed similar to the simple potential. We demonstrate this by measuring the free energy change due to expansion of a system of particles with a LJ potential with a large cutoff radius that is temporarily truncated while the volume changes. This method of free energy calculation reduces computation time by approximately 90% while still producing a free energy difference that is within 3% of that obtained using the LJ potential with the large cutoff radius.

METHOD

To calculate the free energy difference between two states using the JE, the initial state (state 1) must be sampled, before a parametric change to another state (state 2) is carried out using a well-defined protocol, such as a linear decrease in density. The CFT and the MLE also require state 2 to be sampled and the reverse protocol to be considered, taking the system from state 2 to state 1.

A conventional protocol, which we call the Slow Calculation, would simply involve a parametric change in the system from the first to the final state, at the top of Figure 1. The system starts with an initial configuration represented by the point in phase space, $\mathbf{\Gamma}(s) \equiv (\mathbf{q}(s),\mathbf{p}(s))$ which is the full set of particle positions and momentum for all particles. The work for a trajectory of a system that undergoes a parametric change specified through a set of parameters $\boldsymbol{\lambda}_1 \equiv \boldsymbol{\lambda}(0) \rightarrow \boldsymbol{\lambda}_2 \equiv \boldsymbol{\lambda}(t)$ over a period t, which results in the trajectory $\mathbf{\Gamma}(0) \rightarrow \mathbf{\Gamma}(t)$, is given by

$$w_{1\rightarrow 2} = H(\mathbf{\Gamma}(t), \boldsymbol{\lambda}_2) - H(\mathbf{\Gamma}(0), \boldsymbol{\lambda}_1) - Q_{1\rightarrow 2} = \int_0^t \dot{H}^{\mathrm{ad}}(\mathbf{\Gamma}(s), \boldsymbol{\lambda}(s))\, \mathrm{d}s \tag{3}$$

where $H(\mathbf{\Gamma}(0),\boldsymbol{\lambda}_1)$ is the energy of state 1, calculated using its accurate interaction potential, and $H(\mathbf{\Gamma}(t),\boldsymbol{\lambda}_2)$ is the energy of state 2, calculated using its accurate interaction potential. $Q_{1\rightarrow 2}$ is the heat gained by the system during the nonequilibrium process, and $\dot{H}^{\mathrm{ad}}$ is the adiabatic change in the energy (that is, the change in energy excluding heat transfer). In this case, an accurate interaction potential is used for both the sampling of initial points for the transformation trajectories and during the change in system parameters. However, we note that the system is not at equilibrium during the process and that the work is not the reversible work.

Alternatively we can carry out a three-step process that we refer to as the "Fast Calculation," see Figure 1. The steps in the process involve the instantaneous transformation of the interaction potential to one that is significantly more computationally efficient (e.g., truncating a potential) and continuing with whatever parameter change is necessary to drive the system between the two desired states (e.g., expansion) before instantaneously returning the interaction potential to the original, accurate one. The system is out of equilibrium during the process. We will use the parameters $\Phi_A \equiv \Phi(0^-) \rightarrow \Phi_B \equiv \Phi(0^+)$ and $\Phi_B \equiv \Phi(t^-) \rightarrow \Phi_A \equiv \Phi(t^+)$ to represent the change in the interaction potential and $\kappa_1 \equiv \kappa(0) \rightarrow \kappa_2 \equiv \kappa(t)$ to represent the change in the state of the system, so $\lambda \equiv (\kappa,\Phi)$. During each stage, one of the parameters is fixed and the other is varied, allowing eq 3 to be re-expressed as

$$\begin{aligned} w_{1\rightarrow 2} &= \int_{0^-}^{0^+} (\dot{H}(\Gamma(s), \kappa(s), \Phi(s)))\, \mathrm{d}s \\ &\quad + \int_{0^+}^{t^-} (\dot{H}(\Gamma(s), \kappa(s), \Phi(s)))\, \mathrm{d}s \\ &\quad + \int_{t^-}^{t^+} (\dot{H}(\Gamma(s), \kappa(s), \Phi(s)))\, \mathrm{d}s - Q_{0^-\rightarrow 0^+} \\ &\quad - Q_{0\rightarrow t^-} - Q_{t^-\rightarrow t^+} \\ &= H(\Gamma(0), \kappa_1, \Phi_B) - H(\Gamma(0), \kappa_1, \Phi_A) \\ &\quad + H(\Gamma(t), \kappa_2, \Phi_B) - H(\Gamma(0), \kappa_1, \Phi_B) \\ &\quad + H(\Gamma(t), \kappa_2, \Phi_A) - H(\Gamma(t), \kappa_2, \Phi_B) - Q_{1\rightarrow 2} \\ &= H(\Gamma(t), \kappa_2, \Phi_A) - H(\Gamma(0), \kappa_1, \Phi_A) - Q_{1\rightarrow 2} \end{aligned} \tag{4}$$

where Φ_A is the equilibrium interaction potential (the accurate potential) and Φ_B is the nonequilibrium interaction potential (the simple potential). We note that there is no heat exchange due to the instantaneous change in the interaction potential, that is $Q_{0^-\rightarrow 0^+} = Q_{t^-\rightarrow t^+} = 0$.

Comparison of eqs 3 and 4 shows that the formula for the work in the two different transformation algorithms outlined above remains the same. However, note that the value of the work calculated could be very different. For example, if the change in the cutoff radius caused the particles to be in a highly energetically unfavorable state, the work associated with that

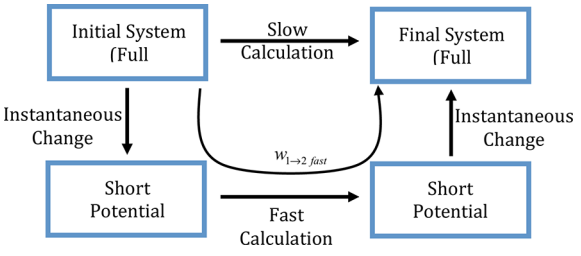

Figure 1. Schematic diagram depicting two pathways for transformation between the initial and final states. Note that the system is only assumed to be at equilibrium when the initial state is sampled.

step would be very high and might not be balanced by the change back after the particles had moved to more energetically favorable configurations. This means that the distributions of work could be quite different in each case, although the JE is still valid. In order to obtain the same level of accuracy using the two protocols, different numbers of samples will be required, with the Slow Calculation approach often likely to have a distribution that produces more accurate predictions of the free energy difference when a finite number of samples are taken. In practice, however, many Fast Calculation samples will be taken for each Slow Calculation sample, and the Fast Calculation approach may provide a more efficient way of obtaining an accurate result. In addition, it may also be possible to design a fast path that has better numerical results than the slow path.

SYSTEM OF INTEREST

To test the proposed algorithm, we consider the change in free energy for a system of thermostatted, LJ particles in a three-dimensional periodic system where the density changes due to linear expansion of the unit cell in one direction in each dimension. MD simulations of this system have demonstrated that the JE can provide accurate calculations of free energy changes, in agreement with equation of state results.[17] In this section, we describe the simulations and how the free energy calculations are carried out.

A convenient technique used to simulate isothermal systems involves the coupling of the system to a Gaussian, isokinetic thermostat.[18] A Gaussian thermostat introduces a Lagrange multiplier to the equations of motion in order to constrain the kinetic energy of the system. Thus, the equations of motion governing the system are

$$\dot{\mathbf{q}} = \mathbf{p}/m$$
$$\dot{\mathbf{p}} = \mathbf{F} - \alpha\mathbf{p} \tag{5}$$

where $\mathbf{q}$ represents the complete set of particle positions, $\mathbf{p}$ represents the complete set of particle momenta, $\mathbf{F}$ represents the complete set of interparticle forces which will depend on the value of the parameter as well as the point in phase space, and α is the Gaussian multiplier for the thermostat, defined as

$$\alpha = \frac{\mathbf{F}\cdot\mathbf{p}}{\mathbf{p}\cdot\mathbf{p}} \tag{6}$$

The heat gained by the system due to the thermostat is

$$Q_{1\to 2} = -2K\int_0^t \alpha(\Gamma(s), \kappa(s), \Phi)\, ds = -3Nk_B T\int_0^t \alpha(\Gamma(s), \kappa(s), \Phi)\, ds \tag{7}$$

where k_B is Boltzmann's constant, T is the system temperature, and N is the number of particles in the system. Therefore, for a system described by the equations of motion 5, undergoing some transformation from state 1 to state 2 by changing λ (the size of the unit cell), the work function of the system is

$$w_{1\to 2} = \int_0^t (\dot{H}(\mathbf{\Gamma}(s), \kappa(s), \Phi))\, ds + 3Nk_B T\int_0^t \alpha(\mathbf{\Gamma}(s), \kappa(s), \Phi)\, ds \tag{8}$$

It should be noted that changing the density within periodic boundary conditions modifies the form of the work relations for this system. The change in the states is due to a parametric change in the volume of the unit cell. It has recently been shown that the JE for this system is[17]

$$\langle e^{-\beta w_{1\to 2}}\rangle_1 = \left(\frac{V_1}{V_2}\right)^N e^{-\beta\Delta F_{1\to 2}} \tag{9}$$

and the MLE relation for the free energy is

$$\sum_{i=1}^{N_{1\to 2}} \frac{1}{1 + \frac{N_{1\to 2}}{N_{2\to 1}}\left(\frac{V_1}{V_2}\right)^N \exp(\beta(w_{1\to 2,i} - \Delta F_{1\to 2}))} = \sum_{i=1}^{N_{2\to 1}} \frac{1}{1 + \frac{N_{2\to 1}}{N_{1\to 2}}\left(\frac{V_2}{V_1}\right)^N \exp(\beta(w_{2\to 1,i} + \Delta F_{1\to 2}))} \tag{10}$$

where V_1 and V_2 are the volumes of the unit cells for the initial and final states and $w_{1\to 2}$ is defined through eq 4 which becomes eq 8 for this thermostatted system. We note that the JE can be applied for the processes $V_1 \to V_2$ and $V_2 \to V_1$ with $\Delta F_{1\to 2} = -\Delta F_{2\to 1}$. If the numerical error in the forward and reverse processes is similar, then

$$\Delta F_{1\to 2} = \frac{1}{2}(\Delta F_{1\to 2} - \Delta F_{2\to 1}) \tag{11}$$

should provide a better estimate of the free energy than is obtained using the results of the JE calculations from just one direction.[7] We refer to eq 9 as a unidirectional JE and the results obtained by combining eqs 9 and 11 as the bidirectional JE.

Fast Calculation Scheme. In a LJ fluid, particles within the system are point masses that interact by the 12−6 LJ pair potential

$$\phi(r_{ij}) = 4\varepsilon\left(\left(\frac{\sigma}{r_{ij}}\right)^{12} - \left(\frac{\sigma}{r_{ij}}\right)^{6}\right) \tag{12}$$

where ε is related to the absolute strength of the potential, r_{ij} is the distance between particle i and particle j, and σ represents the separation at which the potential is zero and can be interpreted as the size of the particles. This potential approaches zero as r_{ij} gets large, so in practice this potential is usually truncated by a cutoff radius, r_{cut}, such that $\phi(r_{ij}) = 0$, $\forall r_{ij} \geq r_{cut}$.

The effects of varying this cutoff radius have been extensively researched for the LJ system.[19,20] In a periodic system with a cubic periodic cell, there is a limit on the cutoff radius that is half the length of unit cell. Increasing the potential cutoff radius to the greatest distance supported by a system's boundary conditions will invariably increase both the accuracy of any resulting calculations and the corresponding calculation time. Here, we can take advantage of our Fast Calculation scheme by instantaneously decreasing the cutoff radius before changing the volume of our unit cell, then instantaneously restoring the cutoff when the final volume is reached. As in eq 4, eq 8 can be expanded

$$w_{1\to 2} = \left(\int_{0^-}^{0^+} (\dot{H}(\mathbf{\Gamma}(s), \kappa(s), \Phi(s)))\, ds\right) + \left(\int_{0^+}^{t^-} (\dot{H}(\mathbf{\Gamma}(s), \kappa(s), \Phi(s)))\, ds\right) + \left(\int_{t^-}^{t^+} (\dot{H}(\mathbf{\Gamma}(s), \kappa(s), \Phi(s)))\, ds\right) + 3Nk_BT\int_0^t \alpha(\mathbf{\Gamma}(s), \kappa(s), \Phi_B)\, ds \quad (13)$$

which can be simplified to give

$$w_{1\to 2} = H(\mathbf{\Gamma}(t), \kappa(t), \Phi_A) - H(\mathbf{\Gamma}(0), \kappa(0), \Phi_A) + 3Nk_BT\int_0^t \alpha(\mathbf{\Gamma}(s), \kappa(s), \Phi_B)\, ds \quad (14)$$

Calculation of eq 14 will be computationally much faster than eq 8 because in the period 0 to t, the interactions between the particles are shorter ranged.

RESULTS

All the simulations consist of two parts: an equilibrium trajectory, run with no parameter change that generates the initial phase points for all the nonequilibrium trajectories, and nonequilibrium trajectories run while changing the cutoff radius and/or expanding/contracting the unit cell. The cutoff radius of the LJ potential used to equilibrate the system is $r_{cut} = 4$, which was shown to give a good estimate of the free energy change due to expansion/contraction using a constant cutoff radius.[17] Three different cutoff radii have been selected for the nonequilibrium transformation component of the simulation for comparative purposes (referred to as the nonequilibrium cutoff radius). The shortest of these, $r_{cut} = (2)^{1/6} \approx 1.122$, produces the Weeks−Chandler−Anderson (WCA) potential, and completely negates the attractive component of the LJ potential.[21] The largest is a cutoff radius of 2.5σ, which is often considered an apt compromise between simulation accuracy and computation speed.[22,23] Finally, a value of 1.6 was chosen between these two values. In addition, Slow Calculations are performed to determine the free energy change for systems with these four cutoff radii, using a nonequilibrium change in the density.

The equations of motion were solved using a fourth order Runge−Kutta algorithm, and cell code was used to increase computational efficiency.[24] All systems simulated underwent both a "forward" change (starting from an equilibrated system with unit cell with sides of length L_1 and changing to length L_2) and a "reverse" change (starting from an equilibrated system with sides of length L_2 and changing to length L_1). All values will be expressed in LJ reduced units. The specific system consisted of 864 particles expanding from a density of $\rho = 0.5$ to $\rho = 0.25$ at a temperature of 1.5.

Quantification of the Error Associated with the Change in Cutoff Radius. In order to quantify the numerical errors that might be expected in the Fast Calculation method due to the sharp, cutoff radius alterations, the behavior of the system when no change in the volume is carried out is initially studied. That is, points are sampled from equilibrium state 1 with a LJ potential with a cutoff radius of 4.0; the potential is then instantaneously changed to have a different cutoff radius. The system is simulated for a period t (with no volume change), and then the potential is instantaneously changed back to the LJ potential with a cutoff radius of 4.0. The unidirectional JE, eq 9, is then used to obtain the free energy change. Figure 2 shows the results of these calculations at a density $\rho = 0.5$. In theory, the free energy change obtained from the unidirectional JE should be zero, so any deviation from that is due to numerical approximations, such as the finite number of samples in the ensemble average. Clearly, the deviation from zero is relatively small in all cases, except when the potential is changed to the WCA potential. Moreover, since the forward and reverse processes are identical, if the bidirectional JE is used to determine the free energy change (eq 11) or the MLE is used (eq 10), the result will be identically zero in all cases. This is an important point for our later calculations where this error can be expected to cancel to some extent.

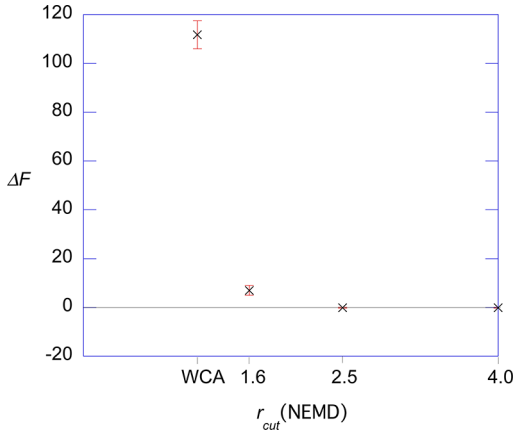

Figure 2. Comparison of the free energy change calculated using the unidirectional JE with $r_{cut} = 4.0$ to sample the initial equilibrium state and various values of r_{cut} for the period $0 \to t$. In this case, there is no volume change during this period, so the theoretical value of the free energy change is zero.

The dominant numerical error in the unidirectional JE calculations is a result of the fact that at the end of the trajectory the distribution function differs from that of state 1 and that the sampling is incomplete. As t increases, the system will have a distribution function that is more and more like the equilibrium distribution of the system with the reduced cutoff radius. Finite sampling means that the rare trajectories that end up at phase points that are unlikely in the WCA system, but likely in state 1, will not be observed even though they could contribute significantly to the average that appears in the JE. This was confirmed by carrying out simulations with various values of t, and it was observed that the error became smaller with shorter t (when the system did not have the opportunity to relax to the WCA equilibrium). Furthermore, as t was increased with the number of samples fixed, the error converged to a fixed value consistent with a final distribution relaxing toward the WCA equilibrium.

It is noted that this is similar to the way in which the error due to sampling in free energy perturbation methods or thermodynamic integration calculations in equilibrium calculations can be estimated from comparing the results obtained from forward and reverse changes.[25]

The results shown in Figure 2 indicate that the unidirectional JE provides estimates of the free energy change to within approximately 10 reduced units of the exact result when the cutoff radius is reduced, except when it is reduced to the WCA potential. This is a valuable result, as the savings in computer time are already substantial when a cutoff radius of 1.6 is used. As discussed above, these numerical errors cancel in application

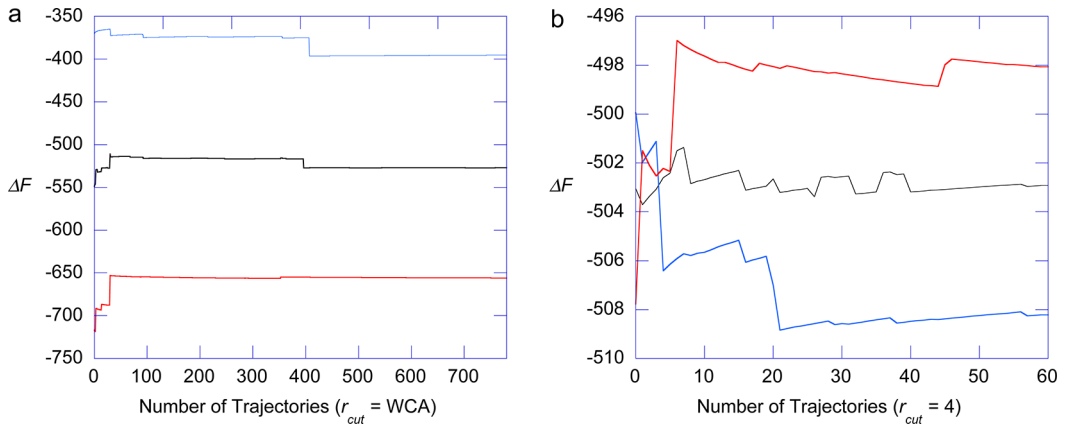

Figure 3. Convergence of the JE and the MLE free energy calculations for transformations between $\rho = 0.5$ and $\rho = 0.25$ for initial and final states with $r_{cut} = 4$ and with the cutoff radii during the change of unit cell volume of r_{cut} = WCA (a) and $r_{cut} = 4$ (b). The blue lines display the results from the JE for the systems undergoing expansion, while the red lines display $-\Delta F$ from the JE for the system being compressed and the black lines give the MLE results.

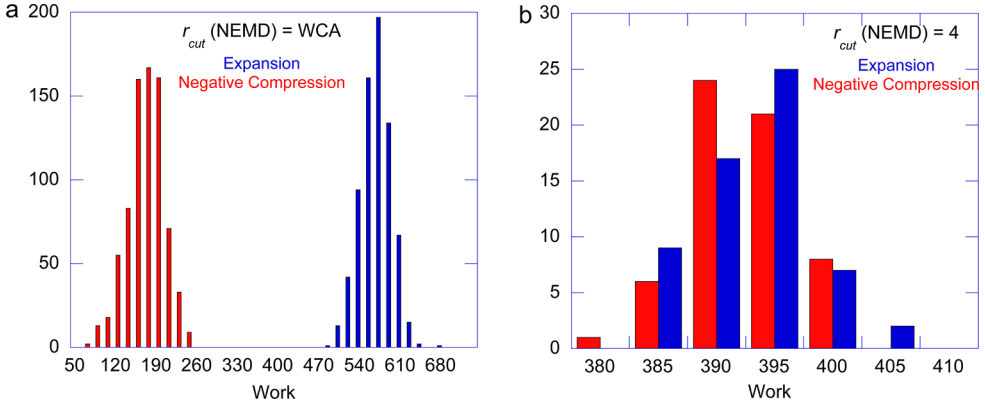

Figure 4. Work distribution profiles of systems undergoing transformations between $\rho = 0.5$ and $\rho = 0.25$ with NEMD cutoff radii of (a) r_{cut} = WCA and (b) $r_{cut} = 4$. The work values represent the $w_{1\to2}$ term of eq 14, and as such do not represent the full contribution to the free energy (see eq 9), with the contribution due to the volume change being approximately −900. The blue bars indicate the work values obtained upon the expansion of the system, while the red bars are $-w_{2\to1}$ for the system undergoing compression.

of the bidirectional JE and the MLE, which will therefore give zero for the free energy change in all cases. Tests at other densities indicate a density dependence of this error, but it is not a strong dependence.

The error that is observed due to the instantaneous change in the cutoff is well understood and could be reduced by introducing intermediates in an optimal way[26] and/or making the change more gradual. However, this would increase the computation time, and our aim is to reduce this while keeping the relative errors in the free energy calculations small. As shown here and below, the error introduced due to the instantaneous change is small in all cases, except when a reduction in the cutoff to the WCA value is carried out, and furthermore the error is canceled to some degree when the forward and reverse processes are considered, so we find it unnecessary to do this.

Computational Test of the Algorithm for Determination of Density Changes. Figure 3 compares the JE and MLE results obtained when the volume is doubled from $\rho = 0.5$ to $\rho = 0.25$ during the period $0 \to t$, in the cases where the cutoff radius is reduced to that of the WCA potential (Figure 3a) and where it is not changed (Figure 3b). The convergence of the two free energy calculation techniques is displayed over an equal CPU time for all of the forward and reverse trajectories, rather than an equal number of time steps. Note the different scales on the ΔF axes. The difference between the JE results for expansion for the two protocols is approximately 110 LJ units, which is consistent with the error shown in Figure 2 for $\rho = 0.5$ with no volume change. Furthermore, the MLE results and the bidirectional JE are indistinguishable, and they are within 10 reduced units of the results obtained when there is no reduction in the cutoff radius. This indicates that the errors due to sampling in the forward and reverse directions are largely canceled. This was expected from the tests carried out for Figure 2. It can be expected that the error due to reducing then increasing the cutoff radius would be similar in the case of expansion and contraction (similar magnitude and same sign), and therefore the errors almost cancel when either the bidirectional JE or the MLE are used. Note that as the MLE works by combining the forward and reverse transformation work results, the MLE free energy changes and the bidirectional JE results require approximately twice as much computation time as the unidirectional JE results displayed for the same number of trajectories.

In Figure 3, we can clearly see the numerical problems of the unidirectional JE discussed above. As the JE is defined through an exponential average (eqs 1 and 9), work values close to and less than the free energy change dominate the average. Thus,

dx.doi.org/10.1021/ct300953u | J. Chem. Theory Comput. 2013, 9, 2083−2089

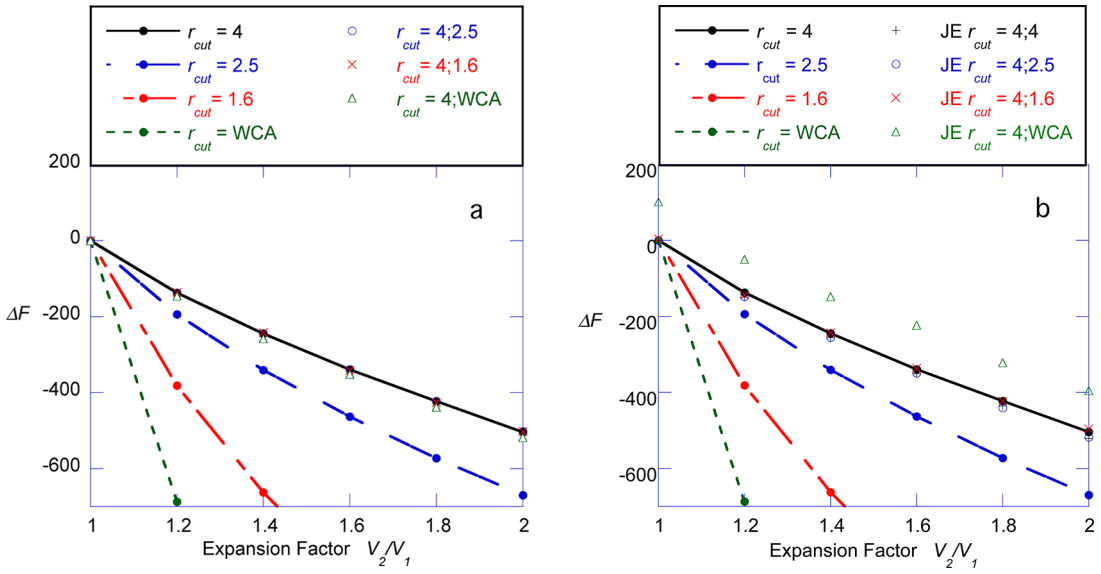

Figure 5. Free energy change for 864-particle LJ system at $\rho = 0.5$ expanding with varying interaction potential cutoffs. In a and b, the lines pass through points (solid circles) obtained from MLE calculations with a constant cutoff radius throughout the simulation and are thus representative of Slow Calculations. The other symbols represent results obtained from the Fast Calculations. In a, the MLE approach was used and gave results that were indistinguishable from the bidirectional JE on the scale shown, and in b, a unidirectional JE was used.

for systems with work distributions insufficiently large to adequately sample the trajectories where $W_{\text{trajectory}} - \Delta F + Nk_BT \ln(V_1/V_2) < 0$, the JE will suffer convergence difficulties.[27] From Figure 3, the value of ΔF is approximately −500 reduced units, so $\Delta F + Nk_BT \ln(V_1/V_2)$ is approximately 400 reduced units. As shown in Figure 4a, the distributions are both well separated from this value, due to the sampling difference between the WCA potential and the potential with $r_{\text{cut}} = 4$, and convergence is extremely poor. In contrast, in Figure 4b, both distributions are clustered around this value, and the unidirectional JE performs well, consistent with the behavior of Figure 3b.

It was found that the unidirectional JE was sensitive to numerical integration errors in calculating the thermostatting multiplier integral. This error arises when taking the difference between a quantity, which is integrated along a trajectory, and a change in the value of the state points at either end of the trajectory (as is done in eqs 8 and 14). It is similar to the "energy error," W_e, of Lechner et al.[16] A small time step (0.001) was used to compare the unidirectional JE and MLE to minimize this error. It was found that for the MLE or the bidirectional JE, the results were not significantly changed when the time step was increased to 0.004, and therefore in the next section this value was used in all calculations.

Comparison of Fast and Slow Calculation Schemes. Ten sets of six forward and six reverse trajectories were used to calculate the free energy difference using both unidirectional JEs, the bidirectional JE, and the MLE, and the results of these simulations are displayed graphically in Figure 5. Each point is calculated with 60 forward and reverse trajectories. The standard error from a set of 10 runs was used to determine the statistical error; however, it is not visible on the scale of Figure 5. The bidirectional JE and MLE results were indistinguishable on the scale shown. The MLE results are also presented numerically in Table 1. The length of all nonequilibrium transformation trajectories was 100 000 time-steps of size 0.004, while the length of the equilibrium trajectories was 5000 timesteps of the same size. Note that the

Table 1. Free Energy Differences and Relative Times Taken for Density Change Simulations with Varying Cutoffs during the Unit Cell Volume Change Dynamics[a]

equilibrium cutoff	dynamics cutoff	free energy change	standard error[b]	relative time taken
4	4	−504.2	0.14%	100%
4	2.5	−502.3	0.11%	28%
4	1.6	−502.6	0.24%	12%
4	WCA	−518.1	0.85%	7.7%
2.5	2.5	−670.3	0.10%	26%

[a]These results were obtained for an 864-particle LJ system undergoing expansion from $\rho = 0.5$ to $\rho = 0.25$. [b]Standard errors were calculated from 10 sets of six free energy changes. The small sample size is the cause of the high variance in these results.

results displayed compare the free energy obtained from a variety of Slow Calculations, with a constant potential cutoff radius throughout the simulation, to the free energy obtained from a variety of corresponding Fast Calculations, where the cutoff radius is reduced for the nonequilibrium transformation.

As can be seen in Figure 5, when constant values of $r_{\text{cut}} = 4$, $r_{\text{cut}} = 2.5$, $r_{\text{cut}} = 1.6$, or $r_{\text{cut}} = (2)^{1/6} = \text{WCA}$ are used throughout the simulation, very different results are obtained for the free energy change. However, in agreement with the theory, simulations where the initial and final states both had $r_{\text{cut}} = 4$, but with a reduced cutoff radius during the nonequilibrium dynamics, all had results within 3% of the constant $r_{\text{cut}} = 4$ simulation when the bidirectional JE or MLE methods were used, as shown in Figure 5a. The greatest reduction in simulation time for the cutoff radii considered was 92.3%. In fact, as shown in Figure 5b, the unidirectional JE also gave good results when $r_{\text{cut}} = 4$, $r_{\text{cut}} = 2.5$, and $r_{\text{cut}} = 1.6$ were used, despite the large changes in the work distributions. Similar results were observed for simulations with initial densities of $\rho = 0.01$ and $\rho = 0.8$. The results for $r_{\text{cut}} = \text{WCA}$ in Figure 5b are shifted by approximately the same amount as in Figure 2 and Figure 3, on the order of 110 reduced units, suggesting that it is caused by the same numerical sampling error.

dx.doi.org/10.1021/ct300953u | J. Chem. Theory Comput. 2013, 9, 2083−2089

The significance of these results can be highlighted by comparing the computational time required to accurately calculate free energy changes of the LJ system with r_{cut} = 4.0. If a highly accurate value of the free energy change of the LJ system is to be obtained, rather than using an r_{cut} = 4.0 for the whole process, accurate results can be obtained using a much smaller r_{cut} during the nonequilibrium process, and this will not result in finite cutoff errors that occur when it is reduced for the whole process. While the Fast Calculation with a nonequilibrium cutoff radius of r_{cut} = 2.5 is actually slightly slower than the Slow Calculation with r_{cut} = 2.5, due to the equilibrium portion of the Fast Calculation being completed with r_{cut} = 4.0, the result is substantially more accurate. Even when the cutoff radius was reduced to r_{cut} = WCA, the worst of the Fast Calculations, the result is still significantly more accurate than the Slow Calculation with r_{cut} = 2.5, and over 3 times faster. This approach therefore seems very valuable for the calculation of free energy changes for interacting particles.

CONCLUSION

In this work, a novel transformation algorithm is proposed and applied to a simple system to give free energy differences which, when compared to the literature standards, are significantly more accurate and are as fast or faster. Use of this algorithm was demonstrated to give results within 3% of the current "high accuracy" results taking only about 8% of the CPU time. The method outlined above is general and robust and can readily be applied to any simulations of free energy changes in which the potential interactions can cause dramatic increases in computation time, for example, simulating phase changes or ionic systems using molecular dynamics. It is also expected to be important in cases where inclusion of fast degrees of freedom in the dynamics or many particle interactions are important to obtain accurate results but are time-consuming and could be neglected during the NEMD step of the process.

The unidirectional JE worked well, with an error that increased with the degree to which the cutoff radius was reduced during the nonequilibrium process. The MLE and bidirectional results were even better, and in this case cancellation of errors in the forward and reverse processes led to excellent results. In some cases, this error might not fully cancel, and this should be tested on a case-by-case basis. Further studies on different systems are underway.

AUTHOR INFORMATION

Corresponding Author

*Phone: +61 7 33463939. Fax: +61 7 33463992. E-mail: D. Bernhardt@uq.edu.au.

Notes

The authors declare no competing financial interest.

ACKNOWLEDGMENTS

The authors thank Owen Jepps for his helpful discussions and insight. Griffith University is acknowledged for computational time on their Cluster and the Australian Research Council for their support. The authors would also like to thank the University of Queensland for computational time on their AIBN Cluster.

REFERENCES

(1) Jarzynski, C. *Phys. Rev. E* **1997**, *56*, 5018−5035.
(2) Jarzynski, C. *Phys. Rev. Lett.* **1997**, *78*, 2690−2693.
(3) It should be noted that when the change in the state of the system occurs sufficiently slowly that the system is at equilibrium at all times, the JE will reduce to $\Delta F_{1\rightarrow 2} = w_{1\rightarrow 2;rev}$ where the subscript "rev" indicates that the path is an equilibrium pathway. When the change in the state of the system is instantaneous, the JE reduces to the free energy perturbation formula $\Delta F_{1\rightarrow 2} = k_B T \ln\langle e^{-\beta(H_2-H_1)}\rangle_1$ where H_1 and H_2 are the internal energies of states 1 and 2, respectively. In both cases, the free energy can be obtained using equilibrium simulations.
(4) Crooks, G. E. *J. Stat. Phys.* **1998**, *90*, 1481−1487.
(5) Crooks, G. E. *Phys. Rev. E* **1999**, *60*, 2721−2726.
(6) Shirts, M. R.; Bair, E.; Hooker, G.; Pande, V. S. *Phys. Rev. Lett.* **2003**, *91*, 140601.
(7) Shirts, M. R.; Pande, V. S. *J. Chem. Phys.* **2005**, *122*, 144107.
(8) Reid, J. C.; Cunning, B. V.; Searles, D. J. *J. Chem. Phys.* **2010**, *133*, 154108.
(9) Vaikuntanathan, S.; Jarzynski, C. *Phys. Rev. Lett.* **2011**, *134*, 054107.
(10) Frenkel, D.; Ladd, A. J. C. *J. Chem. Phys.* **1984**, *81*, 3188−3193.
(11) Mark, A. E.; van Gunsteren, W. F.; Berendsen, H. J. C. *J. Chem. Phys.* **1991**, *94*, 3808−3816.
(12) Eike, D. M.; Brennecke, J. F.; Maginn, E. J. *J. Chem. Phys.* **2005**, *122*, 014115.
(13) Eike, D. M.; Maginn, E. J. *J. Chem. Phys.* **2006**, *124*, 164503.
(14) Grochola, G. *J. Chem. Phys.* **2004**, *120*, 2122−2126.
(15) Zhang, Y.; Maginn, E. J. *J. Chem. Phys.* **2012**, *136*, 144116.
(16) Lechner, W.; Oberhofer, H.; Dellago, C.; Geissler, P. L. *J. Chem. Phys.* **2006**, *124*, 044113.
(17) Davie, S. J.; Reid, J. C.; Searles, D. J. *J. Chem. Phys.* **2012**, *136*, 174111.
(18) Evans, D. J.; Searles, D. J.; Williams, S. R. *J. Chem. Phys.* **2010**, *133*, 104106.
(19) Mastny, E. A.; de Pablo, J. J. *J. Chem. Phys.* **2007**, *127*, 104504.
(20) Palmieri, B.; Ronis, D. *Phys. Rev. E* **2007**, *75*, 011133.
(21) Weeks, J. D.; Chandler, D.; Andersen, H. C. *J. Chem. Phys.* **1971**, *54*, 5237−5247.
(22) Verlet, L. *Phys. Rev.* **1967**, *159*, 98−103.
(23) Smit, B. *J. Chem. Phys.* **1992**, *96*, 8639−8640.
(24) Allen, M. P.; Tildesley, D. J. *Computer Simulations of Liquids*; Clarendon Press: Oxford, 2007.
(25) van Gunsteren, W. F. In *Computer Simulation of Biomolecular Systems: Theoretical and Experimental Applications*; van Gunsteren, W. F., Weiner, P. K., Eds.; Escom Science Publishers: Leiden, The Netherlands, 1989; pp 27−59.
(26) Shenfeld, D. K.; Xu, H.; Eastwood, M. P.; Dror, R. O.; Shaw, D. E. *Phys. Rev. E* **2009**, *80*, 046705.
(27) Jarzynski, C. *Phys. Rev. E* **2006**, *73*, 046105.